

Interfacial Effects of Plasticizers On The Properties of Cellulose Diacetate Materials

Shuaishuai Hu

Nanjing Tech University

Mengting Zhang

Nanjing Tech University

Yufan Wei

Nanjing Tech University

Rui Qi

Nanjing Tech University

Yujia Zhu

Nanjing Tech University

Shuangjun Chen (✉ chenshuangjun@njtech.edu.cn)

Nanjing Tech University <https://orcid.org/0000-0002-9162-6142>

Research Article

Keywords: Cellulose diacetate, Plasticizer, Interface energy, Glass transition temperature, Moisture permeability

Posted Date: October 20th, 2021

DOI: <https://doi.org/10.21203/rs.3.rs-924710/v1>

License: © ⓘ This work is licensed under a Creative Commons Attribution 4.0 International License.

[Read Full License](#)

Interfacial effects of plasticizers on the properties of cellulose diacetate materials

Shuaishuai Hu ^a, Mengting Zhang ^a, Yufan Wei ^a, Rui Qi ^a, Yujia Zhu ^a, Shuangjun Chen

^{a,b,c*}

^aCollege of Material Science & Engineering, Nanjing Tech University, Nanjing, 211816,
Jiangsu, P. R. China;

^b Jiangsu Collaborative Innovation Center for Advanced Inorganic Function
Composites, Nanjing, 211816, P. R. China;

^c Suqian Advanced Materials Institute of Nanjing Tech University, Suqian, 223800,
Jiangsu, P. R. China.

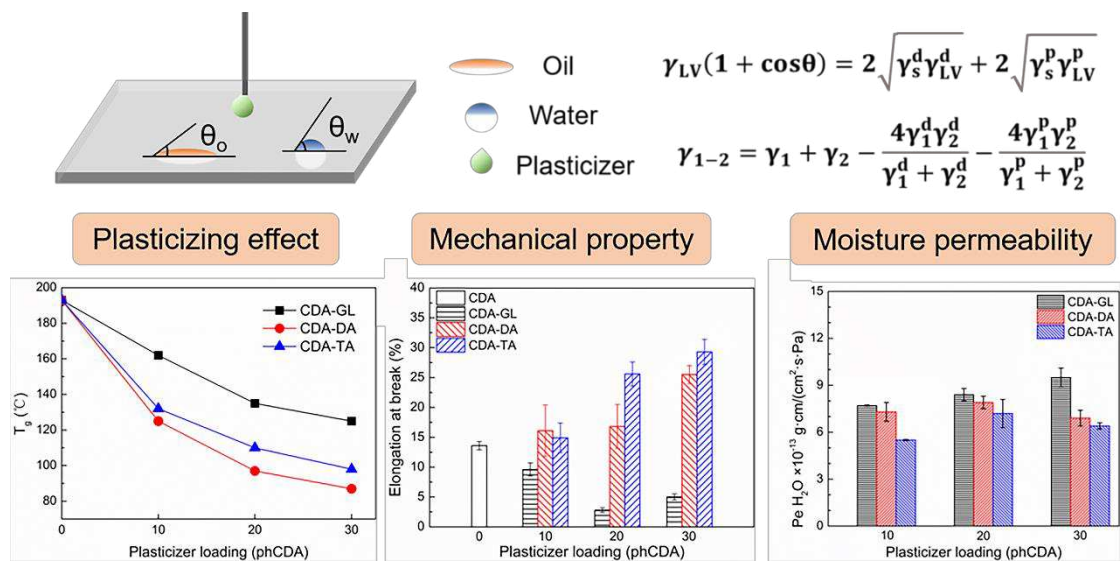
*Corresponding author: chenshuangjun@njtech.edu.cn.

Abstract

Cellulose diacetate (CDA) is a biodegradable biobased polymer, which is not easily melt-processable with a narrow window between flowing and decomposition temperature. Selecting the appropriate plasticizer and evaluating its effect on the properties are important for the application developments of CDA materials. In this paper, eco-friendly plasticizers, such as glycerin (GL), diacetin (DA), triacetin (TA) and polyethylene glycol (PEG) are necessarily introduced. The plasticizing effect is evaluated by harmonic interface energy between CDA and plasticizer from contact angle test. Compared with solubility parameter method, the interfacial method is more effective to estimate PEG with different molecular weight in CDA. Thermal behaviors verify the interfacial method works. Lower interface energy of CDA-DA shows lower glass transition temperature (T_g) determined by differential scanning calorimetry (DSC). Meanwhile, mechanical property, transparency and moisture permeability are all related to the interfacial effects of plasticizers. For instance, the elongation at break of CDA-DA and CDA-TA, which have lower interfacial energy, increase from 14% to 26% and 29%. The CDA-DA and CDA-TA films also have high visible light transmittance about 90%. The moisture permeability of plasticized CDA film increases with the decreased interface energy between water and plasticizer. Interfacial method provides a new route for preparing high-performance CDA materials.

Keywords Cellulose diacetate; Plasticizer; Interface energy; Glass transition temperature; Moisture permeability

35 **Graphical abstract**



36

37

Introduction

Cellulose is the quintessential sustainable resource and the most abundant natural polymer on the earth (Cheng et al. 2016; Huang et al. 2021; Peng et al. 2020) and has attracted much attention due to its unique derivable structure and biodegradability (Schurz 1999; Wang et al. 2017). Cellulose diacetate (CDA) as an important cellulose ester is available at industrial scale (Rustemeyer 2004; Simon et al. 1998; Wang et al. 2018), and usually applied for manufacturing CDA fiber through wet spinning process from its acetone solution (Cho et al. 2013; Edgar et al. 2001). CDA is not easily melt-processable by conventional extrusion or injection processes (Boulven et al. 2019), because it has a high glass transition temperature (T_g) and a narrow window between flowing temperature (T_f) and decomposition temperature (T_d) (Benazzouz et al. 2017; Iji et al. 2013). From this perspective, plasticizers are necessarily introduced to disrupt strong dipolar interaction network, improving the CDA chain activity. CDA is normally plasticized by citrates, phthalates, glycerin derivatives, etc. Among them, phthalate esters have been subjected to environmental scrutiny as a health threat (Vu Thanh et al. 2014). Additionally, the migration of undesirable plasticizer could cause serious hazards to health and environment (Ghiya et al. 1996; Quintana et al. 2012). Thus, the precise choice of green plasticizers makes the thermoplastic development a daunting task for CDA materials (Li et al. 2018).

Cellulose acetate has the hygroscopic behavior due to the presence of hydroxyl groups in their chemical structure (Chen et al. 2020; Khoshtinat et al. 2021; Lovikka et al. 2018), could be applied for moisture-permeable films. Manon Boulven et al. (2019)

used a large number of acylated aliphatics to produce a series of cellulose mixed esters, found that the water transport mainly depends on the water solubility. The water solubility is inversely related to the alkane chain length of the acylated aliphatic and the degree of acylation. A.A. Al-Hassan et al. (2012) separately incorporated two plasticizers, glycerin and sorbitol, into fish gelatin-sago starch films. It is found that plasticizers can improve the dense polymer molecular chain network structure and increase the free volume, which leads to the film is more susceptible to moisture permeability. As for the mechanical properties of CDA materials, Vu Thanh Phuong et al. (2014) used diacetin and triacetin as plasticizers and blended them with CDA in order to obtain rigid or semi-rigid plastic samples with high toughness.

The fundamental method to evaluate the plasticizing effect is exploring the compatibility between plasticizer and polymer. When analyzing the compatibility between multiphase, the solubility parameter method principle of "similar in cohesive energy density or solubility parameter (δ)" is usually accepted. A. Greco et al. (2010) used Hansen solubility parameter to correlate the miscibility of polyvinyl chloride and plasticizer to the chemical structure of plasticizer. Jarod M. Younker et al. (2016) obtained Hildebrand and Hansen solubility parameters from simulations on pure single-component systems to quantify the compatibility between plasticizer and polymer. Nevertheless, the solubility parameter method has shortcomings when applied to complex systems (Betron et al. 2017).

Herein, an interfacial method was introduced to evaluate the plasticizing effect based on contact angle test and interface energy calculation. Glycerin (GL), diacetin (DA),

triacetin (TA) and polyethylene glycol (PEG) were chosen as the green candidate plasticizers for CDA. The differential scanning calorimetry (DSC) was applied to detect the evolutions of T_g and melting temperature (T_m), which quantify the plasticizing effect. The dynamic mechanical thermal analysis (DMTA) was used to investigate the modulus change with temperature. In addition, the mechanical properties of plasticized CDA were measured by tensile test. The transparency and moisture permeability of plasticized CDA film was monitored by UV-Visible spectrophotometer and moisture-permeable cup.

Experimental Section

Materials

Cellulose diacetate (CDA, degree of acetyl substitution: 2.45) was supplied by Nantong Cellulose Fibers Co., Ltd. (Nantong, China). Glycerin (GL) was purchased from Sinopharm Chemical Reagent Co., Ltd. (Shanghai, China). Diacetin (DA) and triacetin (TA) were purchased from Tianjin Heowns Biochemical Technology Co., Ltd. (Tianjin, China). Polyethylene glycol with average molecular weight of 1000 and 2000 g/mol (PEG1 and PEG2) were purchased from Dalian Meilun Biotechnology Co., Ltd. (Dalian, China). Tetrahydrofuran (THF) was provided by Wuxi City Yasheng Chemical Co., Ltd. (Yixing, China). These reagents were used as received.

Fabrication of films

Thin films of CDA and polystyrene (PS) were prepared by spin coating for contact angle test. The microscope coverslip was cut into square as film carrier. CDA and PS were separately dissolved in THF to prepare solution with a mass concentration of 0.5%.

The speed of Spin Coater (WS-650Mz-23NPPB, Laurell, USA) was set to 800 r/min and the running time was 35 s. In addition, Coatings of PEG1 and PEG2 were prepared from 5% THF solution on the coverslip by roller coating for contact angle test. The roll speed of small automatic coating machine (XT-200CA, OSP, China) was set as 70 mm/s. The above films and coatings were baked in a vacuum oven at 60 °C for 4 h.

CDA films containing different type and dosage of plasticizers (GL, DA, TA, PEG1 and PEG2) were prepared by solution casting. THF was used as a solvent and solution mass concentration was 10%. The loading of plasticizer was set at 0, 10, 20 and 30 **phCDA (parts per hundred CDA)**. CDA was sufficiently dissolved in an environment of 25 °C by a magnetic stirrer. The homogeneous solution was cast in a petri dish and the solvent was evaporated in a fume hood and a vacuum oven of 80 °C. Finally, the samples for different characterization tests were cut out.

The moisture-permeable films of CDA plasticized by GL and its derivatives were prepared by Elcometer Film Applicator. The coating liquids were the same as the above casting solutions. After the solution was fully volatilized, several films of a certain area (8×8 cm²) were cut out for water vapor permeability test.

Characterization

The contact angles of different liquids on the coated films were recorded by a contact angle measuring instrument (DSA100, Krüss, Germany) under the environment of 18±2 °C and 30±2 %RH. Water, paraffin oil and liquid plasticizers (GL, DA and TA) were dropped on the PS and CDA films. Water and diiodomethane were dropped on the PEG1 and PEG2 coatings. These contact angles were obtained at 15 s. The non-polar

and polar surface energy parameters of water, paraffin oil and diiodomethane were listed in Table 1.

Table 1. The surface energy parameters of water, paraffin oil and diiodomethane

Liquid	γ_{LV} (mJ·m ⁻²)	γ_{LV}^d (mJ·m ⁻²)	γ_{LV}^p (mJ·m ⁻²)
Water	72.8	21.8	51.0
Paraffin oil	30.7	30.7	0
Diiodomethane	50.8	49.5	1.3

γ_{LV} The surface energy of liquid, γ_{LV}^d The non-polar surface energy of liquid, γ_{LV}^p The polar surface energy of liquid.

The thermal analysis was performed on a DSC instrument (Q20, TA, USA). The sample was placed in sealed aluminium crucible. The plasticized CDA was heated from 40 °C to 220 °C (two heating cycles) and then cooled down from 220 °C to 40°C (one cooling cycle). The procedure was executed with a temperature ramp of 10 °C/min under nitrogen atmosphere. The T_g is determined from the heating run and positioned by the half-height method. The T_m is located at the top of melting peak. The ΔH_m is calculated based on the area of melting peak. The DMTA test was carried out with torsion mode on a modular compact rheometer (MCR302, Anton paar, Austria) to detect modulus change with temperature. The average dimension of samples was 20×8×0.5 mm³. The test was performed at 1 Hz and the torsion amplitude is 0.1%. Sample was heated from 40 °C to 170 °C at a heating rate of 4 °C/min.

The tensile test was performed on a universal testing machine (CMT 5254, SANS, China). The average size of samples was 50×5×0.5 mm³ and the stretching rate was 5

mm/min. The visible light transmittance of CDA film was obtained from Ultraviolet-Visible spectrophotometer (UV3200, Mapada, China). The spectra were recorded from 800 to 200 nm and the scan step was 1 nm. The moisture permeability of CDA film was tested by a moisture-permeable cup. The cup was filled with moderate amount of distilled water. The interface between film and cup was sealed with silicone rubber. The test was carried out in an oven at 60 °C for 4 h and the weight loss (Δm) was recorded. The moisture permeability coefficient ($P_{e\ H_2O}$) of film was calculated according to the Eq. (1).

$$P_{e\ H_2O} = \frac{\Delta m \times d}{S \times t \times P} \quad (1)$$

where d is the film thickness, S is the mouth area of moisture-permeable cup, t is test time, P is the water vapor pressure.

Results and discussion

Solubility parameter method

Solubility parameter method is widely applied for the plasticizing effect evaluation. We operated the following calculations by referring to the A. Greco's method (Greco et al. 2010; Van Krevelen and Te Nijenhuis 2009). The solubility parameters of CDA and plasticizers can be achieved as follow:

$$\delta = (\delta_d^2 + \delta_p^2 + \delta_h^2)^{0.5} \quad (2)$$

where δ_d is the contribution of dispersion forces, δ_p is the contribution of polar forces, δ_h is the contribution of hydrogen bonding. A combination contribution of dispersion and polar forces is introduced:

$$\delta_v = (\delta_d^2 + \delta_p^2)^{0.5} \quad (3)$$

The interaction radius (IR) between CDA and plasticizer can be obtained as:

$$IR = ((\delta_{v,CDA} - \delta_{v,plasticizer})^2 + (\delta_{h,CDA} - \delta_{h,plasticizer})^2)^{0.5} \quad (4)$$

Table 2. Solubility parameter terms and interaction radius (IR) for the plasticizers and CDA

Material	δ (J·cm ⁻³) ^{0.5}	δ_v (J·cm ⁻³) ^{0.5}	δ_h (J·cm ⁻³) ^{0.5}	IR (J·cm ⁻³) ^{0.5}
CDA	20.8	16.3	12.9	--
GL	35.5	20.8	28.7	16.4
DA	22.9	17.3	15.0	2.3
TA	19.9	16.8	10.6	2.4
PEGs	23.7	21.8	9.3	6.6

Table 2 lists the different solubility parameter and the IR calculated according to Eq. (4). DA have the lowest IR, suggesting that it is the most suitable plasticizer probably. TA has almost the same IR, slightly higher than DA. The GL's IR is extremely the highest (~16.4), indicating that it is the most unsuitable plasticizer. PEG was applied to plasticize CDA as reported by P. R. Rao et al. (1997). The IR of PEGs is 6.6. According to the solubility parameter method, PEGs with different molecular weight have the same plasticizing effect.

Interfacial method

Table 3 lists the contact angles of different liquids on the CDA, PS, PEG1 and PEG2. The contact angles of water on the PS and CDA are 95.9° and 69.2°, suggesting the polarity of CDA is higher than that of PS. The contact angles of GL, DA and TA on the PS decrease successively with 86.0°, 45.9° and 36.0°. This is because the polarity decreases with the increasing ratio of ester group. The contact angles of water on the

PEG1 and PEG2 are 6.5° and 6.9°, which are closer to each other. However, diiodomethane contact angles of PEG1 and PEG2 have relatively large difference. This indicates that the interface energies are different for different molecule weight PEGs with CDA.

Table 3. The contact angle (CA) of different liquids on the CDA, PS, PEG1 and PEG2

Type	CA-W ^a (°)	CA-O ^{b1} (°)	CA-O ^{b2} (°)	CA-GL (°)	CA-DA (°)	CA-TA (°)
CDA	69.2	16.7	--	70.1	11.7	6.4
PS	95.9	15.7	--	86.0	45.9	36.0
PEG1	6.5	--	4.9	--	--	--
PEG2	6.9	--	12.5	--	--	--

^a Water, ^{b1} Paraffin oil, ^{b2} Diiodomethane.

The polar and non-polar surface energies of CDA, GL, DA and TA were calculated according to the Eq. (5) based on the contact angle data (Kobayashi et al. 2012; Owens and Wendt 1969; Zhang et al. 2019).

$$\gamma_{LV}(1 + \cos\theta) = 2\sqrt{\gamma_s^d\gamma_{LV}^d} + 2\sqrt{\gamma_s^p\gamma_{LV}^p} \quad (5)$$

where θ is contact angle of droplet on the film, γ_s^d and γ_s^p are non-polar and polar surface energies of film.

The interface energy between CDA and plasticizer was calculated according to the Eq. (6) (Biresaw and Carriere 2002).

$$\gamma_{1-2} = \gamma_1 + \gamma_2 - \frac{4\gamma_1^d\gamma_2^d}{\gamma_1^d + \gamma_2^d} - \frac{4\gamma_1^p\gamma_2^p}{\gamma_1^p + \gamma_2^p} \quad (6)$$

where γ_{1-2} represents the interface energy between CDA (1) and plasticizer (2). γ_1 , γ_1^d and γ_1^p are surface energy, non-polar and polar surface energies of CDA. γ_2 , γ_2^d

and γ_2^p are surface energy, non-polar and polar surface energies of plasticizer.

Fig. 1 gives the surface energies of CDA, GL, DA, TA, PEG1, PEG2 independently and their interface energies of CDA-GL, CDA-DA, CDA-TA, CDA-PEG1, CDA-PEG2. In Fig. 1a, the surface energies of CDA and DA are both about $40 \text{ mJ}\cdot\text{m}^{-2}$, close to each other. The polar surface energy of DA is also close to that of CDA. The interface energy of CDA-DA is the lowest ($2.00 \text{ mJ}\cdot\text{m}^{-2}$), which is consistent with the IR value by solution parameter method. We can suppose that lower interface energy suggests the better plasticizing effect of CDA-DA. As for CDA-PEG in Fig. 1b, the surface energy of PEG is much greater than that of CDA. Thus, the interface energy between PEG and CDA is large. Evaluated by the interfacial method, the plasticizing effect of PEG1 is a little better than that of PEG2.

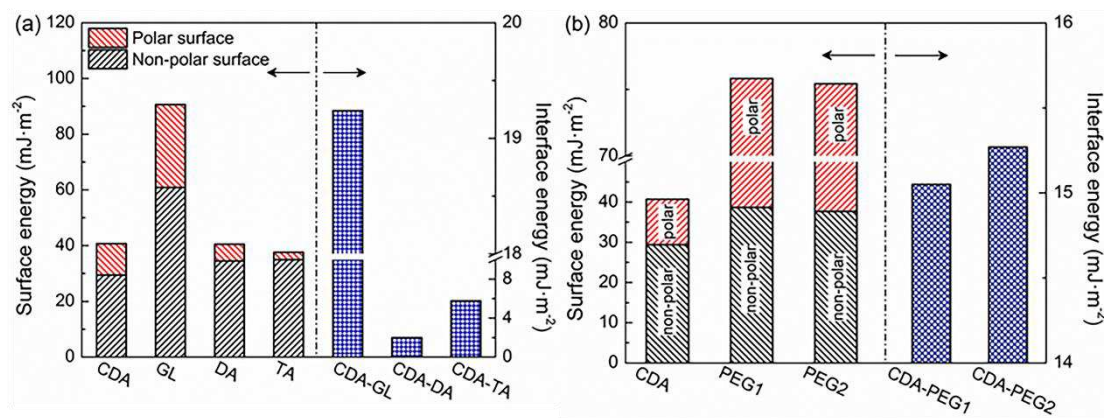


Fig. 1. (a) The surface energies of CDA, GL, DA, TA and the interface energies of CDA-GL, CDA-DA, CDA-TA; (b) The surface energies of CDA, PEG1, PEG2 and the interface energies of CDA-PEG1, CDA-PEG2

Thermal behaviors

Fig. 2 shows the second heating cycle in DSC for some samples and the changes in T_g and T_m of plasticized CDA. A small amount (10 phCDA) of plasticizer incorporated

can lead to a significant decline in T_g and T_m as shown in Fig. 2a. The hydroxyl or ester groups in plasticizers undermine the strong interaction and increase the "free volume" between CDA molecular chains, reducing the activation energy for the coordinated movement of CDA molecular chains (Vu Thanh et al. 2014). T_g decreases from 193 °C for pure CDA to 87 °C for CDA-DA, and to 98 °C for CDA-TA, and to 125 °C for CDA-GL in Fig. 2b. Such a decrease degree of T_g is ascribed to the plasticizing effect. Therefore, CDA-DA has the best plasticizing effect, which is consistent with the result evaluated by the interfacial method. In Fig. 2c, the T_m of CDA-GL solely drops to about 210 °C, which shows that GL is a poor plasticizer for CDA. Both DA and TA can effectively reduce the T_m , so that we can process CDA materials at a lower temperature without severe thermal degradation.

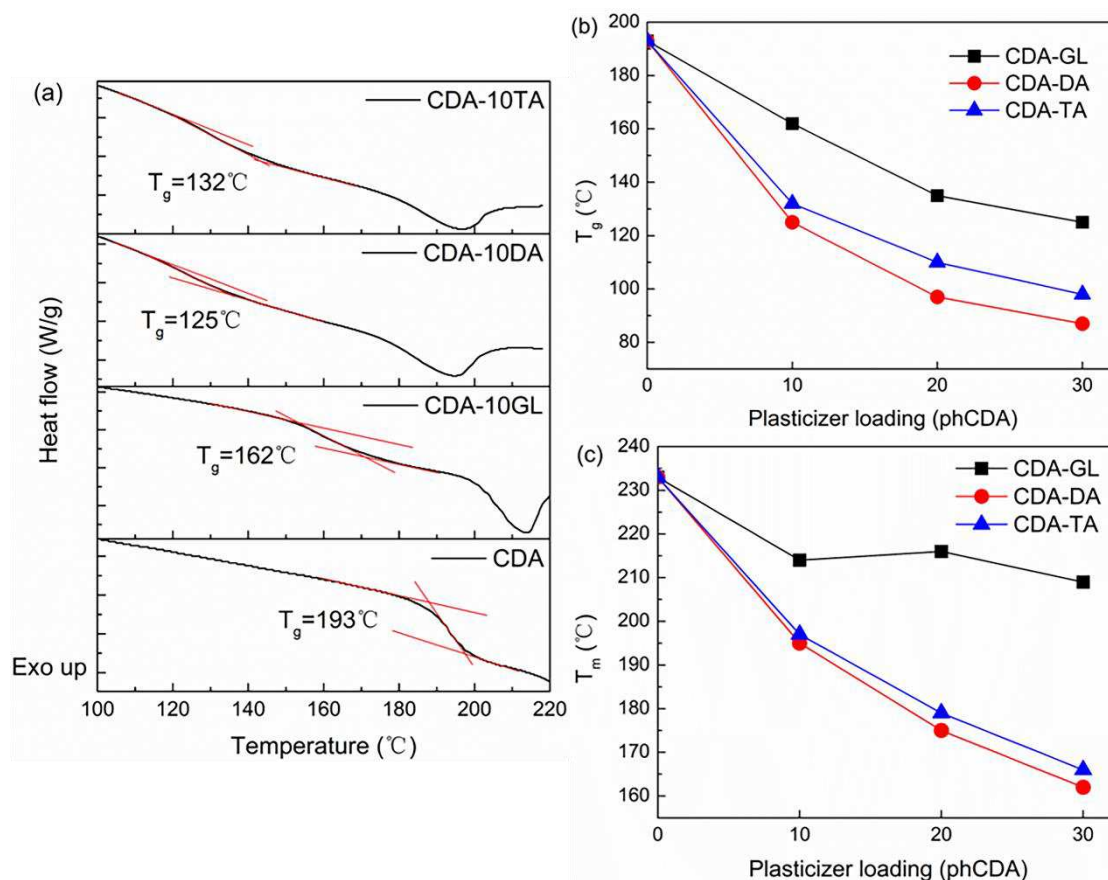


Fig. 2. (a) DSC curves of CDA, CDA-10GL, CDA-10DA and CDA-10TA; Evolution of (b) T_g and (c) T_m as a function of the plasticizer loading

Fig. 3 shows the storage modulus (G') as a function of temperature for plasticized CDA. In Fig. 3b and Fig. 3c, the turning point of G' curve, the soften temperature point, significantly shifts to the low temperature region with the increase in plasticizer loading, which is different from that of CDA-GL in Fig. 3a. The G' curves of CDA-DA and CDA-TA also drop notably at high temperature, because DA and TA make the CDA molecular chain "soft" effectively. These demonstrate that DA and TA have excellent plasticizing roles on CDA, as suggested by interfacial energies. Meanwhile, the G' of CDA-DA is higher than that of CDA-TA under high temperature. This is because DA has strong polarity and forms intense stickers (Xavier Dreux 2019) between CDA molecular chains.

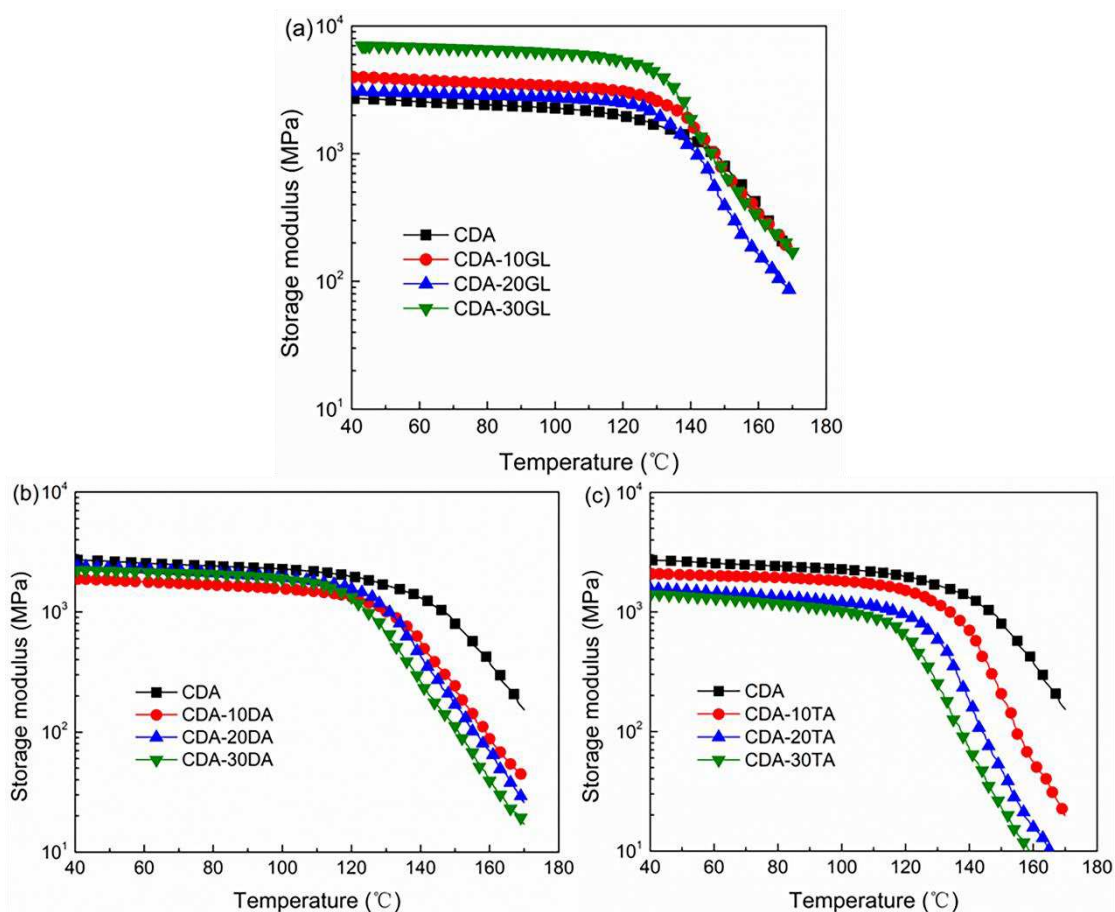


Fig. 3. Storage modulus (G') vs. the temperature for (a) CDA-GL, (b) CDA-DA and (c) CDA-TA

In Fig. 4, the DSC and DMTA are also used to determine the plasticizing effect of PEG for CDA. According to Fig. 4a, the T_m of CDA-PEG rises with the addition of PEG content, indicating that both PEG1 and PEG2 have poor plasticizing effects on CDA. Furthermore, the T_m of CDA-PEG1 is lower than that of CDA-PEG2, regardless of PEG content is 10 phCDA or 30 phCDA. In Fig. 4b, the modulus decreases slowly, reflecting the compatibility of PEG with CDA is worse than DA and TA. Despite this, due to the diluting effect of PEG in the CDA matrix, the increase in PEG content leads to a decrease in the initial modulus. Differently, as the temperature increases, the G' curve of CDA-PEG2 decreases less. Thus, the plasticizing effect of PEG2 is worse than that of PEG1, which is accordance with the evaluation result of interfacial method.

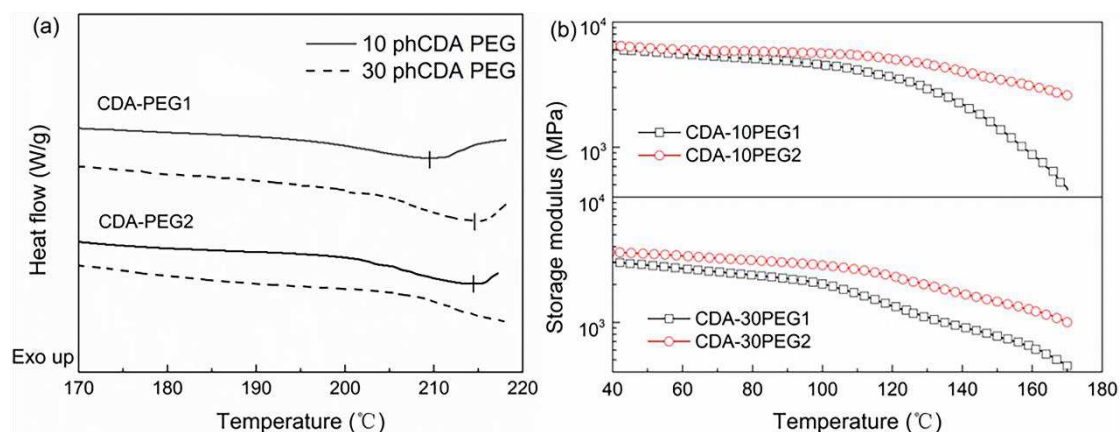


Fig. 4. (a) DSC curves of CDA-PEG1 and CDA-PEG2; (b) Storage modulus (G') curves of CDA-PEG1 and CDA-PEG2

Mechanical properties

Fig. 5 reveals the tensile strength and the elongation at break of plasticized CDA. In Fig. 5a, no matter which plasticizer is selected for CDA, the tensile strength generally decreases as the plasticizer content increases (Muscat et al. 2012). At the same plasticizer content, the tensile strength of CDA-DA is weaker than that of CDA-TA. This is because DA has higher polar surface energy, which forcefully destroy the dipolar interaction network between CDA molecular chains. The elongation at break in Fig. 5b is a key indicator to inspect the plasticizer effectiveness. For the CDA-GL, the elongation at break becomes low due to the incompatibility between them. On the contrary, as the content of DA or TA increases, the elongation at break improves, which indicates that both DA and TA have better compatibility with CDA. When the plasticizer amount is 30 phCDA, the elongation at break of CDA-DA and CDA-TA can reach to 26% and 29%, respectively.

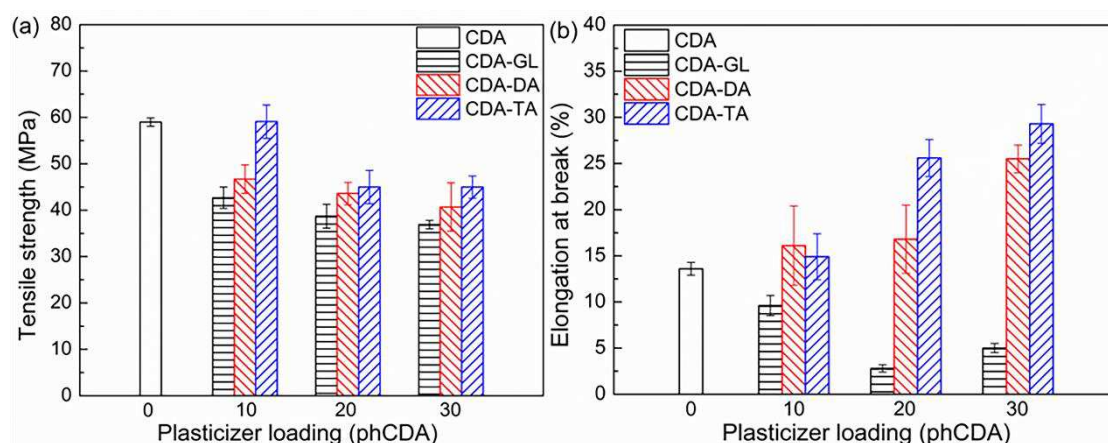


Fig. 5. (a) The tensile strength and (b) the elongation at break of plasticized CDA

Moisture permeability

The moisture permeability of plasticized CDA films was measured to evaluate the influence of plasticizer on water transport performance. Generally, the $P_{e\ H_2O}$ proceeds through a solution-diffusion mechanism, that is the product of the solubility S of permeate by its diffusion coefficient D (Fick's first law). Polymer chain must “move aside” to open up the water transportation path (Boulven et al. 2019). Also, note that the moisture permeability test was conducted at 60 °C, which can neglect the plasticizing effect. Diffusion coefficient is thus mainly limited by the crystallinity, which is reflected in the ΔH_m (Fig. 6b). Meanwhile, the solubility is governed by the hydrophilicity of plasticizer, that is the interface energy between plasticizer and water (Fig. 6a). Fig. 6d shows that the $P_{e\ H_2O}$ of CDA-GL is higher than that of CDA-DA and CDA-TA. It improves with the GL content increasing, which is ascribed to the GL's high hydrophilicity and the continuous crystallinity decline. For CDA-DA and CDA-TA, the $P_{e\ H_2O}$ firstly increases and then decreases. From 10 to 20 phCDA, the crystallinity significantly reduces and this influence far offsets the increased hydrophobicity. From 20 to 30 phCDA, the crystallinity almost no longer decreases,

but the plasticizer content increases, which causes the hydrophilicity deterioration. In this frame, CDA-30DA is the ideal candidate to prepare high moisture permeability film.

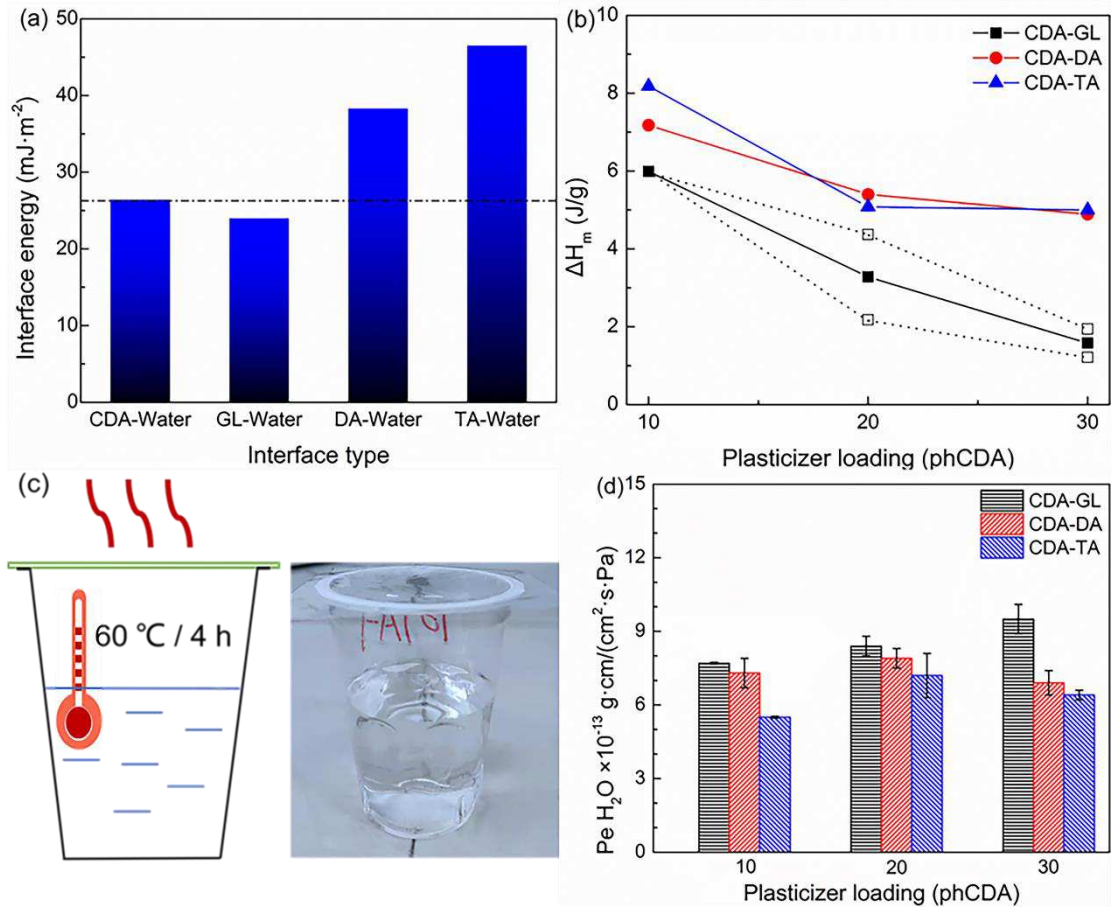


Fig. 6. (a) The interface energies of CDA and plasticizer with water based on the surface energies in the section of *interfacial method*; (b) The ΔH_m of plasticized CDA film in the first heating cycle of DSC; (c) The photo of a moisture-permeable cup; (d) The $P_e H_2O$ of plasticized CDA film

Transparency

The optical transmittance data between the wavelength of 800 and 200 nm for three plasticized CDA films has been exhibited in Fig. 7. Evaluated by the interfacial method, the compatibility between CDA and plasticizer is ranked as follow: CDA-DA > CDA-TA >> CDA-GL. If GL is used to plasticize CDA, it will cause phase separation and

migrate to film surface (Martino et al. 2006; Tsou et al. 2014). Correspondingly, the film of CDA-30GL has the low visible light transmittance with 11.5%. In contrast, the transparency of CDA-30DA and CDA-30TA is very high, which shows that DA and TA have better compatibility with CDA. Moreover, this excellent transparency is mainly owing to a large number of amorphous structures existed in CDA (Wang et al. 2018).

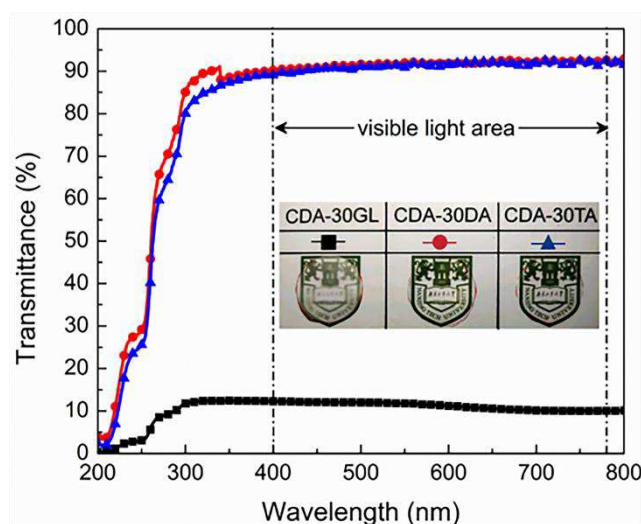


Fig. 7. The UV-vis transmittance curves of CDA moisture-permeable films over a range of 200-800 nm

Conclusion

In this study, interfacial method based on the harmonic interface energy is introduced to evaluate plasticizing effect of eco-friendly CDA materials. The interface energy between CDA and DA is the lowest ($2.00 \text{ mJ} \cdot \text{m}^{-2}$). When the DA content is 30 phCDA, the T_g and T_m of CDA reduce to 87°C and 162°C , which is the best plasticizing effect among glycerin and its derivatives. The evaluation results of the interfacial method are in line with the actual plasticizing effects. Meanwhile, according to the plasticizing effect of PEG with different molecular weight on CDA, the interfacial method is slightly better than the solubility parameter method. As for other properties, they are

also closely related to the interfacial effects of plasticizers. Due to CDA-TA has lower interface energy and TA has not high polarity, CDA-30TA has strong and tough mechanical properties, with the tensile strength and elongation at break are 45 MPa and 29%. Thanks to the high hydrophilicity of GL, CDA-30GL has an outstanding moisture permeability coefficient ($\sim 9.5 \times 10^{-13} \text{ gH}_2\text{O} \cdot \text{cm}/(\text{cm}^2 \cdot \text{s} \cdot \text{Pa})$). CDA-DA and CDA-TA also show high transparency because of their low interface energy.

Acknowledgments We are grateful to Industry Prospect and Common Key Technology of Suqian Science and technology plan (No. H201815) for financial support of this work. We give great thanks to a project funded by the Priority Academic Program Development of Jiangsu Higher Education Institutions (PAPD) and Jiangsu Students' Platform for Innovation and Entrepreneurship Training Program (202010291103Y).

Declarations

Conflict of interest The authors declare no competing financial interest.

References

- Al-Hassan AA, Norziah MH (2012) Starch–gelatin edible films: Water vapor permeability and mechanical properties as affected by plasticizers. *Food Hydrocolloid* 26:108-117. <http://doi.org/10.1016/j.foodhyd.2011.04.015>
- Benazzouz A, Dudognon E, Correia NT, Molinier V, Aubry J-M, Descamps M (2017) Interactions underpinning the plasticization of a polymer matrix: a dynamic and structural analysis of DMP-plasticized cellulose acetate. *Cellulose* 24:487-503. <http://doi.org/10.1007/s10570-016-1148-y>
- Betron C, Bounor-Legare V, Pinel C, Scalabrino G, Djakovitch L, Cassagnau P (2017) Diffusion of modified vegetables oils in thermoplastic polymers. *Mater Chem Phys* 200:107-120. <http://doi.org/10.1016/j.matchemphys.2017.07.059>
- Biresaw G, Carriere CJ (2002) Interfacial tension of poly(lactic acid)/polystyrene blends. *J Polym Sci Pol Phys* 40:2248-2258. <http://doi.org/10.1002/polb.10290>
- Boulven M, Quintard G, Cottaz A, Joly C, Charlot A, Fleury E (2019) Homogeneous acylation of Cellulose diacetate: Towards bioplastics with tuneable thermal and water transport properties. *Carbohydr Polym* 206:674-684. <http://doi.org/10.1016/j.carbpol.2018.11.030>
- Chen Q et al. (2020) Hygroscopic swelling of moso bamboo cells. *Cellulose* 27:611-620. <http://doi.org/10.1007/s10570-019-02833-y>

- Cheng Qiaoyun, Chang Chunyu, Zhang Lina (2016) Progress in tunicate cellulose based advanced functional materials. *Scientia Sinica Chimica* 46:438-451.
- Cho M, Oh YI, Nam JD, Lee Y (2013) Influence of elastomeric core-shell impact modifiers on mechanical properties of cellulose diacetate resin. *Cellulose* 20:3239-3245. <http://doi.org/10.1007/s10570-013-0046-9>
- Dreux X, Majeste JC, Carrot C, Argoud A, Vergelati C (2019) Viscoelastic behaviour of cellulose acetate/triacetin blends by rheology in the melt state. *Carbohydr Polym* 222. <http://doi.org/10.1016/j.carbpol.2019.114973>
- Edgar KJ, Buchanan CM, Debenham JS, Rundquist PA, Seiler BD, Shelton MC, Tindall D (2001) Advances in cellulose ester performance and application. *Prog Polym Sci* 26:1605-1688. [http://doi.org/10.1016/S0079-6700\(01\)00027-2](http://doi.org/10.1016/S0079-6700(01)00027-2)
- Ghiya VP, Dave V, Gross RA, McCarthy SP (1996) Biodegradability of cellulose acetate plasticized with citrate esters. *J Macromol Sci A*. A33:627-638. <http://doi.org/10.1080/10601329608010883>
- Greco A, Brunetti D, Renna G, Mele G, Maffezzoli A (2010) Plasticizer for poly(vinyl chloride) from cardanol as a renewable resource material. *Polym Degrad Stabil* 95:2169-2174. <http://doi.org/10.1016/j.polymdegradstab.2010.06.001>
- Huang D et al. (2021) Top-down fabrication of biodegradable multilayer tunicate cellulose films with controlled mechanical properties. *Cellulose*. <http://doi.org/10.1007/s10570-021-04161-6>
- Iji M, Toyama K, Tanaka S (2013) Mechanical and other characteristics of cellulose ester bonded with modified cardanol from cashew nut shells and additional aliphatic and aromatic components. *Cellulose* 20:559-569. <http://doi.org/10.1007/s10570-012-9832-z>
- Khoshtinat S, Carvelli V, Marano C (2021) Moisture absorption measurement and modelling of a cellulose acetate. *Cellulose* 28:9039-9050. <http://doi.org/10.1007/s10570-021-04114-z>
- Kobayashi M, Terayama Y, Yamaguchi H, Terada M, Murakami D, Ishihara K, Takahara A (2012) Wettability and Antifouling Behavior on the Surfaces of Superhydrophilic Polymer Brushes. *Langmuir* 28:7212-7222. <http://doi.org/10.1021/la301033h>
- Li DY, Panchal K, Mafi R, Xi L (2018) An Atomistic Evaluation of the Compatibility and Plasticization Efficacy of Phthalates in Poly(vinyl chloride). *Macromolecules* 51:6997-7012. <http://doi.org/10.1021/acs.macromol.8b00756>
- Lovikka VA, Rautkari L, Maloney TC (2018) Changes in the hygroscopic behavior of cellulose due to variations in relative humidity. *Cellulose* 25:87-104. <http://doi.org/10.1007/s10570-017-1570-9>
- Martino VP, Ruseckaite RA, Jiménez A (2006) Thermal and mechanical characterization of plasticized poly (L-lactide-co-D,L-lactide) films for food packaging. *J Therm Anal Calorim* 86:707-712. <http://doi.org/10.1007/s10973-006-7897-3>
- Muscat D, Adhikari B, Adhikari R, Chaudhary DS (2012) Comparative study of film forming behaviour of low and high amylose starches using glycerol and xylitol as plasticizers. *J Food Eng* 109:189-201. <http://doi.org/10.1016/j.jfoodeng.2011.10.019>
- Owens DK, Wendt RC (1969) Estimation of the surface free energy of polymers. *J Appl Polym Sci* 13:1741-1747. <http://doi.org/10.1002/app.1969.070130815>
- Peng N, Huang D, Gong C, Wang YX, Zhou JP, Chang CY (2020) Controlled Arrangement of Nanocellulose in Polymeric Matrix: From Reinforcement to Functionality. *Acs Nano* 14:16169-16179. <http://doi.org/10.1021/acsnano.0c08906>
- Quintana R, Persenaire O, Bonnaud L, Dubois P (2012) Recent advances in (reactive) melt processing of cellulose acetate and related biodegradable bio-compositions. *Polym Chem-UK* 3:591-595.

- <http://doi.org/10.1039/c1py00421b>
- Rao P R, Diwan P V (1997) Permeability studies of cellulose acetate free films for transdermal use: influence of plasticizers. *Pharmaceutica acta Helvetiae* 72:47-51. [http://doi.org/10.1016/S0031-6865\(96\)00060-X](http://doi.org/10.1016/S0031-6865(96)00060-X)
- Rustemeyer P (2004) *Cellulose Acetates: Properties and Applications*, Heidelberg (Germany), 2003 - Preface. *Macromolecular Symposia* 208.
- Schurz J (1999) 'Trends in polymer science'-A bright future for cellulose. *Prog Polym Sci* 24:481-483. [http://doi.org/10.1016/S0079-6700\(99\)00011-8](http://doi.org/10.1016/S0079-6700(99)00011-8)
- Simon J, Muller HP, Koch R, Muller V (1998) Thermoplastic and biodegradable polymers of cellulose. *Polym Degrad Stabil* 59:107-115. [http://doi.org/10.1016/S0141-3910\(97\)00151-1](http://doi.org/10.1016/S0141-3910(97)00151-1)
- Tsou CH et al. (2014) Preparation and Characterization of Bioplastic-Based Green Renewable Composites from Tapioca with Acetyl Tributyl Citrate as a Plasticizer. *Materials* 7:5617-5632. <http://doi.org/10.3390/ma7085617>
- Van Krevelen DW, Te Nijenhuis K (2009) Cohesive Properties and Solubility. In: Van Krevelen DW, Te Nijenhuis K (eds) *Properties of Polymers*, 4rd edn. Elsevier, Amsterdam, pp 189-227.
- Phuong VT, Verstichel S, Cinelli P, Anguillesi I, Coltelli M-B, Lazzeri A (2014) Cellulose Acetate Blends - Effect of Plasticizers on Properties and Biodegradability. *J Renew Mater* 2:35-41. <http://doi.org/10.7569/JRM.2013.634136>
- Wang WC, Li FX, Yu JY, Wang HB (2017) Coagulation studies for hydroxyethyl cellulose (HEC) in NaOH/H₂O solvent. *Fiber Polym* 18:1091-1097. <http://doi.org/10.1007/s12221-017-1000-5>
- Wang W, Liang T, Bai HY, Dong WF, Liu XY (2018) All cellulose composites based on cellulose diacetate and nanofibrillated cellulose prepared by alkali treatment. *Carbohydr Polym* 179:297-304. <http://doi.org/10.1016/j.carbpol.2017.09.098>
- Younker JM, Poladi RH, Bendler HV, Sunkara HB (2016) Computational screening of renewably sourced polyalkylene glycol plasticizers for nylon polyamides. *Polym Advan Technol* 27:273-280. http://doi.org/10.1002/pat.3632_1
- Zhang XQ, Mao ZP, Zhang J (2019) Study of the phase morphology and toughness in poly (vinyl chloride)/acrylonitrile-styrene-acrylic/styrene-butadiene-styrene ternary blends influenced by interfacial/surface tension. *J Appl Polym Sci* 136. <http://doi.org/10.1002/app.47721>

Supplementary Files

This is a list of supplementary files associated with this preprint. Click to download.

- [Graphicalabstract.tif](#)